

Effects of Gas-mixed Electrolyte on Leveling Ability of Electrochemical Machining of ($\gamma+\alpha_2+B_2$) TiAl Intermetallic

Yaowu Zhou, Di Zhu*, Zhengyang Xu, XiFang Zhang

Di Zhu, College of Mechanical and Electrical Engineering, Nanjing University of Aeronautics & Astronautics, P.O. Box1005, 29 Yudao St., Nanjing 210016, China;

*E-mail: dzhu@nuaa.edu.cn

Received: 19 February 2020 / Accepted: 9 April 2020 / Published: 10 June 2020

Genetic error is an important factor that affects the electrochemical machining (ECM) accuracy of ($\gamma+\alpha_2+B_2$) TiAl intermetallic. Investigations have shown that the effect of genetic error can be reduced by appropriately increasing the leveling ratio. This study aimed to improve the leveling ability by using gas-mixed electrolyte. A high-speed camera was employed to observe the bubble distribution of the gas-mixed electrolyte in the machining gap. Experimental investigations verified that the leveling ratio increased from 0.49 to 0.74 as the void fraction increased from 0% to 70% and almost increased by 51% with the gas mixed into the electrolyte during ECM. Furthermore, the surface roughness value changed from 0.6481 to 0.2682 when the void fraction varied from 0% to 70%, implying that the use of gas-mixed electrolyte during ECM improves the surface quality of a workpiece.

Keywords: ECM, gas-mixed electrolyte, leveling ability

1. INTRODUCTION

ECM is a non-traditional machining method that selectively removes material from a workpiece based on the electrochemical anodic dissolution principle. Owing to its main advantages of high acceleration efficiency, final workpiece surface quality, and low tool electrode loss, ECM is receiving increased attention and has been used in a wide range of applications such as aerospace parts, high-end medical equipment, and other fields [1].

ECM is an effective method for profile machining. However, genetic errors left on a machined workpiece surface often exist because of the uneven blank allowance in electrolytic profile machining, particularly in the initial stage of processing. The ability to eliminate allowance differences depends on the leveling ability of the ECM. When the leveling ability is high, the ability to eliminate allowance difference is high; when the leveling ability is low, the ability to eliminate allowance difference is low [2]. Therefore, the effect of genetic error can be effectively reduced by increasing the leveling ability. In

ECM, the leveling ability refers to the ability to eliminate the difference between the maximum and the minimum allowances. The stronger the leveling ability, the faster the difference between the maximum and the minimum allowances is eliminated and the lesser the influence of genetic error [3]. Various approaches have been developed to improve the leveling ability and enhance the localization of anodic dissolution. Rajurkar [4] set up a model to predict the minimum allowance of ECM, and the simulation results showed that a passivation electrolyte and pulse current minimized material removal, improved the machining accuracy, and reduced the amount of electrolytic product used. Zhu [3] analyzed the effects of machining parameters on leveling ability, and the experimental results indicated that the leveling ratio was improved by using a higher pulse frequency and a lower pulse duty and applied voltage. Li [5] presented an electrochemical micromachining method that utilized a combination of side-insulated electrodes, cathode and anode micro-gap control, and pulse current machining to demonstrate the feasibility of electrochemical micromachining and its potential for improving machining accuracy and reducing machining size. Bahre [6] obtained a higher material removal rate in a small machining gap and a lower material removal rate in large machining gap with a good leveling ratio that achieved higher machining localization and machining accuracy. Qian [7] applied an auxiliary anode in ECM to significantly improve the machining localization, and the etch factor was decreased with an increase in the machining voltage.

The effects of gas-mixed electrolyte in ECM have been researched. Li [8] established simulation models of gas-mixed and non-gas-mixed electrolyte flow fields of ECM, and the simulations showed that the flow field distribution of gas-mixed electrolyte on the workpiece surface was more uniform, the eddy current region was greatly restricted, and the flow field was significantly improved. Hu [9] proposed a new method for decreasing the stray corrosion in trepanning ECM, in which air was supplied around the machined workpiece to remove stray electrolyte, and the electrolyte became oxygen-enriched by the mixing of the oxygen and the electrolyte. Ayyappan [10] presented ECM experiments using an oxygen-enriched electrolyte and found that oxygen-enriched electrolyte improved the material removal rate and achieved good surface quality.

$(\gamma+\alpha_2+B_2)$ TiAl intermetallic is a relatively new material, and because of its excellent high-temperature strength, high modulus, creep resistance, oxidation resistance, and flame-retardant properties, it has been gradually applied to aero-engine blades, diffusers, and other components [11]. The allowance difference for machining these parts is large because of the complex structure of these components. The allowance difference must be eliminated when the minimum allowance is processed. Thus, it is necessary to improve the leveling ability of ECM. Therefore, the leveling ability of $(\gamma+\alpha_2+B_2)$ TiAl intermetallic in ECM was studied, experimental research was conducted, and the leveling ability of ECM was improved by the use of gas-mixed electrolyte. The gas-mixed electrolyte flow field was observed to analyze the distribution of bubbles in the machining gap, and it was important to concentrate on the relationship between the void fraction and the leveling ratio. In this study, the effects of gas-mixed electrolyte in ECM on the leveling ability of $(\gamma+\alpha_2+B_2)$ TiAl intermetallic were investigated. A high-speed camera was used to observe the bubble distribution of gas-mixed electrolyte in the machining gap.

2. PRINCIPLE OF ECM PROCESS FOR A STEPPED SURFACE WITH LEVELING ABILITY

To explore the influence of gas-mixed electrolyte on leveling ability, $(\gamma+\alpha_2+B2)$ TiAl intermetallic with a stepped surface was used as the anode workpiece. The schematic diagram of the leveling process of the stepped workpiece is illustrated in Fig. 1. The leveling ratio, Ψ , represents the leveling ability and is defined as

$$\psi = \frac{\delta_0 - \delta_b}{h}, \tag{1}$$

where δ_0 is the initial stepped height difference, δ_b is the final stepped height difference, and h is the dissolved depth. In Fig. 1, A_{max} represents the largest workpiece allowance and A_{min} the smallest. After a short time t , the A_{max} with the largest allowance becomes $A_{max,t}$, and the A_{min} with the smallest allowance becomes $A_{min,t}$. In this way, the parameters in Eq. (1) can be expressed as

$$\psi = 1 - \frac{\int_0^t v_{min} dt}{\int_0^t v_{max} dt}. \tag{2}$$

To improve the leveling ratio, it is necessary to increase the difference of the dissolution rate at different allowances from Eq. (2); therefore, the dissolution rate becomes faster when the allowance is large and slower when the allowance is small.

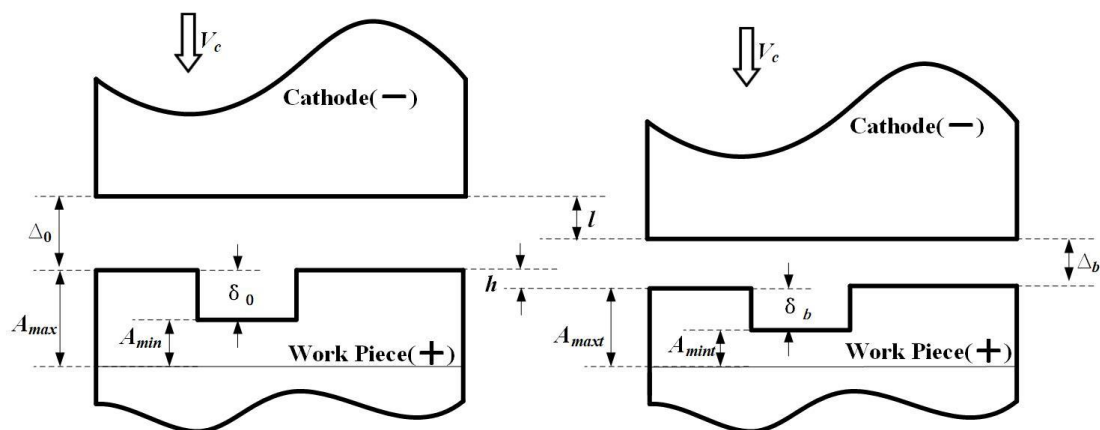


Figure 1. Schematic diagram of leveling process of stepped workpiece.

According to the Faraday's law, the dissolution rate v_t is defined as

$$v_t = \eta \omega \kappa \frac{U_R}{\Delta_x}, \tag{3}$$

where η represents the electrolyte efficiency, ω is the volume electrochemical equivalent, κ is the electrolyte conductivity, Δ_x is the machining gap, and U_R is the voltage applied between the electrodes.

The relationship between the electrolyte, κ , and the void fraction, β , is

$$\kappa = \kappa_0 [1 + \xi(T - T_0)] (1 - \beta)^n, \tag{4}$$

where κ_0 is the initial electrolyte conductivity, and T and T_0 represent the outlet and inlet electrolyte temperatures, respectively. The gas-mixed electrolyte in ECM has a greater effect on electrolyte conductivity than that of electrolyte temperature [12].

The gas-mixed electrolyte is defined as

$$\beta = \frac{Q_g}{Q_g + Q_l} \times 100\%, \tag{5}$$

where Q_g is the gas volume, and Q_l is the liquid volume.

Gas–liquid two-phase flow with a uniform mixture is a bubble flow. In a bubble flow, the bubbles are surrounded by liquid and are an independent individual [12]. Therefore, the flow velocity of the gas is equal to the flow velocity of the liquid, and the mechanical energy of the gas does not change.

According to the law of conservation of mechanical energy, the mechanical energy of gas E^Q can be expressed as

$$E^Q = E_K^Q + E_P^Q = \text{Constant}, \quad (6)$$

$$E_P^Q = E_G^Q + E_E^Q, \quad (7)$$

where E_K^Q is the kinetic energy of gas, E_P^Q is the potential energy of gas, E_G^Q is the gravitational potential energy of gas, and E_E^Q is the elastic potential energy of gas.

Without considering E_G^Q , combining Eq. (6) and Eq. (7) obtains

$$E^Q = E_K^Q + E_E^Q = \text{Constant}. \quad (8)$$

In gas–liquid two-phase flow, the flow conforms to the principle of fluid continuity and can be expressed as

$$\rho v S = \text{Constant}, \quad (9)$$

where ρ is the flow density, v is the flow velocity, and S is the cross-sectional area of the flow.

According to Eq. (9), flow velocity is inversely proportional to the cross-sectional area of the flow; therefore, the velocity of gas is inversely related to the gap. When the gap increases, the velocity of the gas decreases, E_K^Q decreases, and E_E^Q increases; when the gap decreases, the velocity of gas increases, E_K^Q increases, and E_E^Q decreases.

In gas–liquid two-phase flow, the pressure inside the bubbles and the pressure of the liquid are in a state of dynamic equilibrium and determines the volume of the bubbles. When the equilibrium is changed, the relative change in E_E^Q and E_E^L will determine the direction of equilibrium movement. Liquid is considered to be incompressible. Therefore, the elastic potential energy of a liquid E_E^L will not change in a flow field. Hence, the change in bubble volume is positively correlated with the change in E_E^Q .

When the gap increases, E_E^Q increases, the bubble volume increases, and the conductivity of the electrolyte decreases. When the gap decreases, E_E^Q decreases, the bubble volume decreases, and the conductivity of the electrolyte increases. According to Eq. (3), the dissolution rate is proportional to the conductivity of the electrolyte. Hence, in gas-mixed ECM, when the gap decreases, the dissolution rate increases; and when the gap increases, the dissolution rate decreases. Thus, the dissolution rate difference at different machining gaps in gas-mixed ECM is larger than that of traditional ECM. In summary, the gas-mixed electrolyte can improve the leveling ability of ECM.

3. EXPERIMENTAL INVESTIGATIONS

The system schematic of the gas-mixed electrolyte flow in ECM is shown in Fig. 2. It consisted of electrodes, a power supply, gas circulating equipment, and an electrolyte circulating system. The gas was precisely mixed into the electrolyte by an air compressor under the control of throttle valves and flow meters. To investigate the effects of gas-mixed electrolyte during ECM, the machining process was observed by a high-speed camera as shown in Fig. 3.

In this investigation, ($\gamma+\alpha_2+B_2$) TiAl intermetallic and stainless steel were employed as the anodic workpiece and the cathode, respectively. The anodic workpiece was a 30-mm square blank with a stepped surface as shown in Fig. 4. The step height difference between the higher and lower surfaces was 1 mm. The stainless-steel cathodic electrode tool was flat and square with a side length of 30 mm. The fixture model and its physical object which is made of insulating material are illustrated in Fig. 5.

The machining conditions in the experiments are illustrated in Table 1. The profile of the machined anode was examined by hex three coordinate measurement (Letiz Reference HP, Germany), and the surface topographies of the partial samples were measured using a three-dimensional profiler (DVM5000, Leica, Germany).

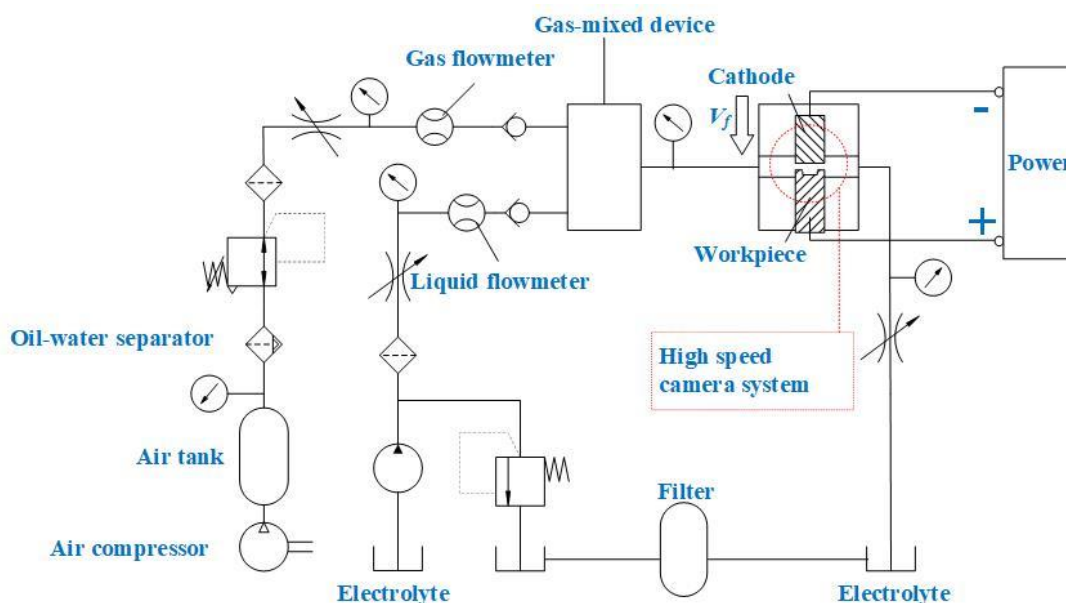


Figure 2. Schematic diagram of gas-mixed ECM.

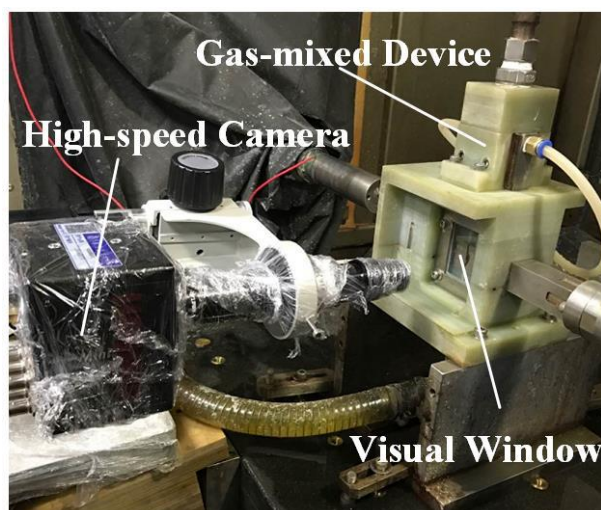


Figure 3. Illustration of high-speed camera setup.

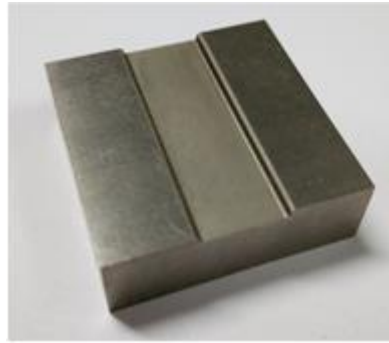


Figure 4. Image of TiAl anode workpiece with stepped surface.

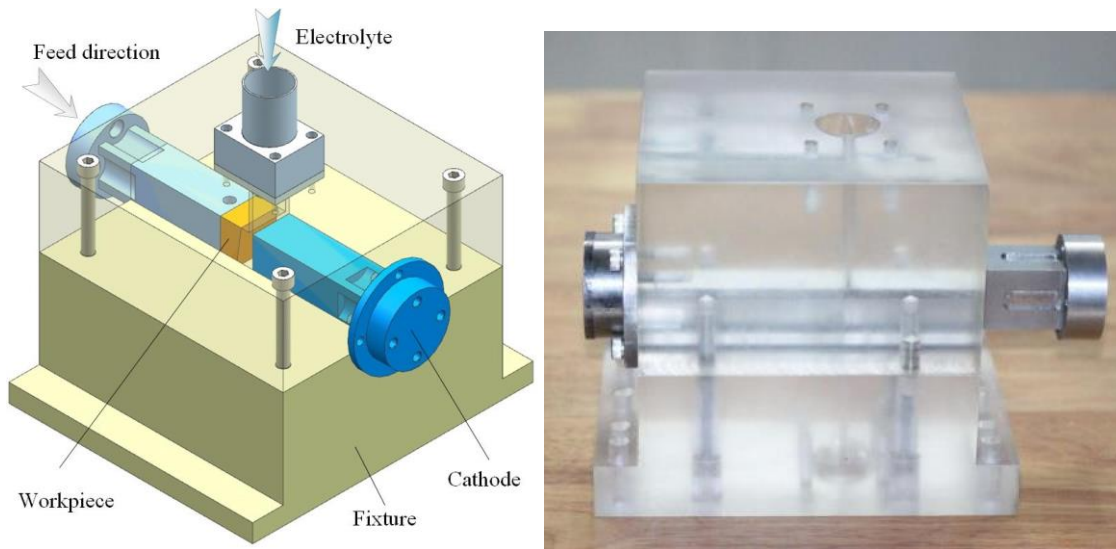


Figure 5. Fixture model and real object of the experiment

Table 1 Machining conditions

Parameter	Value
Anode workpiece	($\gamma+\alpha_2+B2$) TiAl intermetallic
Cathode workpiece	Stainless steel
Step height difference, δ_0	1 mm
Cathode feed rate, v_c	0.9 mm min ⁻¹
Cathode feed distance, l	1 mm
Initial machining gap, Δ_0	0.6 mm
Applied voltage, U_R	30 V
Pulse duty cycle	80%
Pulse frequency, f	100 Hz
Electrolyte conductivity, κ_0	20% NaNO ₃ (15 S/m)
Inlet pressure, P_I	0.8 MPa
Outlet pressure, P_O	0.1 MPa
Electrolyte temperature, T	30 °C
Range of void fraction, β	0/0.1/0.2/0.3/0.4/0.5/0.6/0.7

4. RESULTS AND DISCUSSION

4.1 High-speed camera observations

Advanced measurement technology is helpful for understanding the machining principle. Klocke recorded the ECM process of Inconel 718 using the optical in situ measurements of a high-speed thermography camera. These measurements provided a deeper understanding of the process and served as input and validation for an interdisciplinary process simulation model based on conservation equations [13].

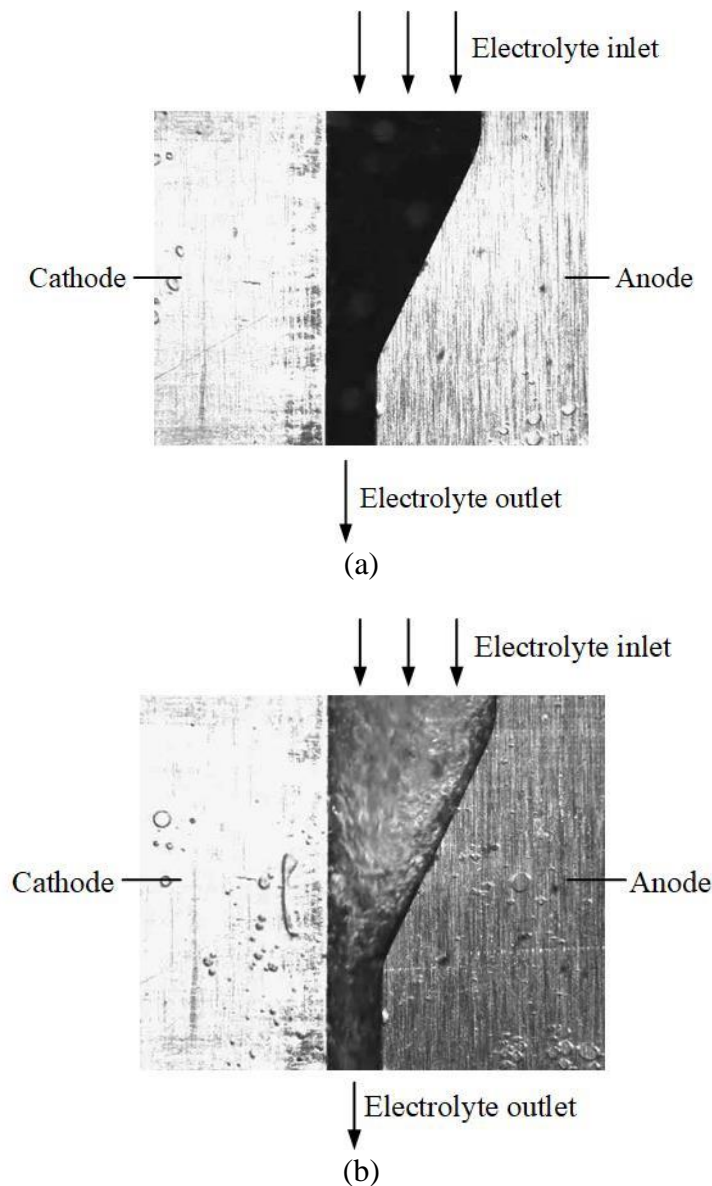


Figure 6. High-speed camera images of electrolyte flow pattern in machining gap: (a) non-gas-mixed electrolyte flow, and (b) gas-mixed electrolyte flow.

The images of the electrolyte flow pattern in the machining gap captured by the high-speed camera are displayed in Fig. 6. As shown in Fig. 6(a), when the electrolyte was not mixed with gas, there

was no reflection of bubbles in the gap, and the gap image appeared black. As shown in Fig. 6(b), when the electrolyte was mixed with gas, a large number of bubbles existed in the gap, and the gap image was much brighter. In the gap, the bubbles were evenly and densely distributed in the electrolyte, the liquid-phase fluid was continuous, and the gas-phase fluid was dispersed. As a result, the flow pattern of the gas–liquid two-phase flow was a bubble flow.

The shooting area of the high-speed camera was narrowed to clearly observe the gas-mixed flow field. Fig. 7(a) is an enlarged view of the electrolyte flow at a large gap, and Fig. 7(b) is an enlarged view of the electrolyte flow at a small gap.

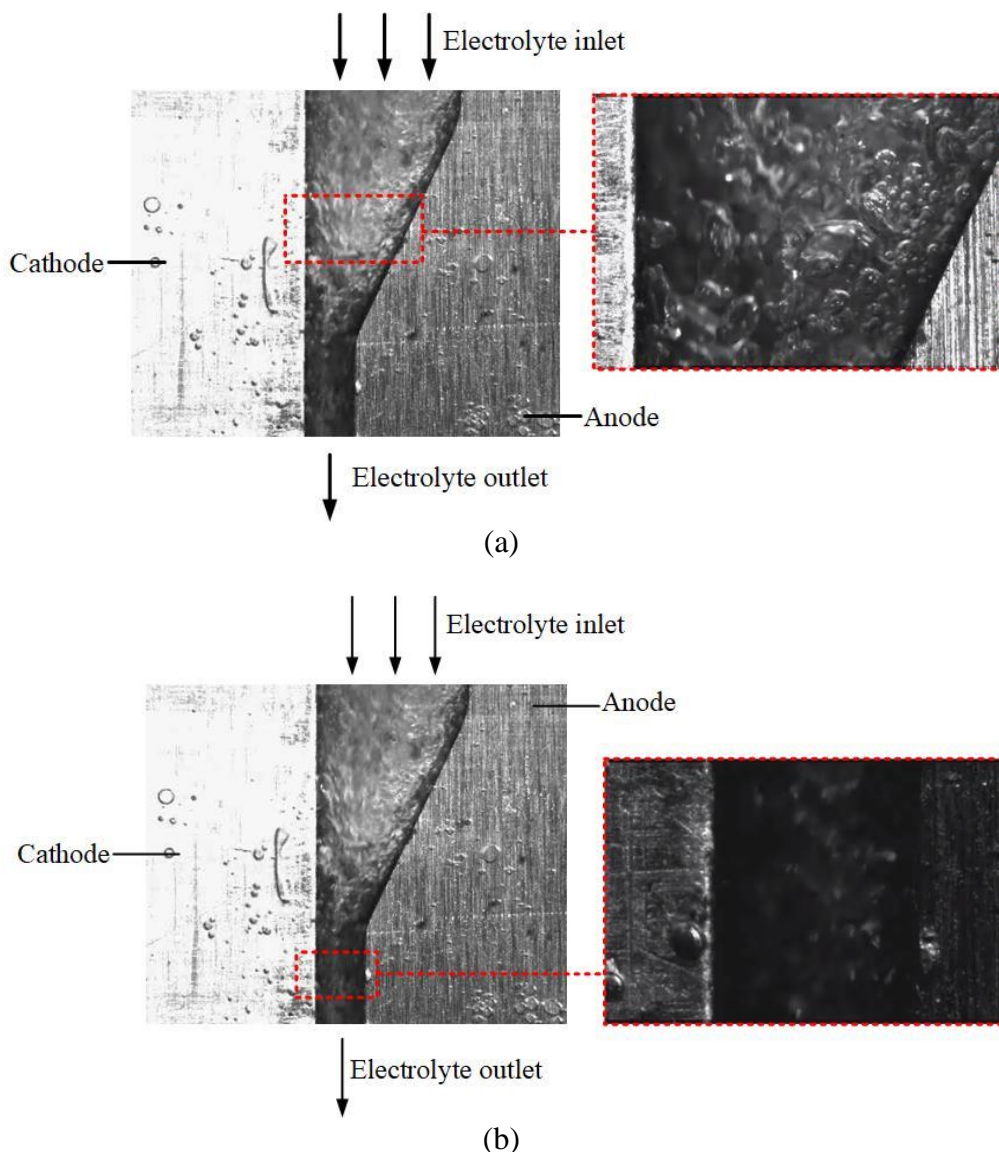


Figure 7. Enlarged views of gas-mixed electrolyte flow in: (a) a large gap, (b) a small gap.

The diameter of bubbles in the regions with large gaps was generally larger than that in the regions with small gaps. Mechanical energy consists of kinetic and potential energy; therefore, because the velocity of a bubble is inversely related to the gap size, the velocity of a bubble at a large gap is low, and the kinetic energy of the bubble is small. According to the conservation of mechanical energy, when

the kinetic energy is smaller at the large gap, the potential energy is correspondingly higher. For a bubble, the elastic potential energy increases without considering the gravitational potential energy, and the volume of the bubble is proportional to the elastic potential energy. Therefore, the bubble volume is large at a large gap and small at a small gap.

Above all, larger bubbles at large gaps lead to more distorted and longer field lines. At the same time, the void fraction is relatively higher at large gaps, resulting in relatively low conductivity; therefore, the electrolytic reaction speed at large gaps is slower than that at small gaps and improves the leveling ability.

To investigate the effect of gas-mixed electrolyte flow on ($\gamma+\alpha_2+B2$) TiAl intermetallic during the ECM process, the void fraction changed by adjusting the gas flow rate and the electrolyte rate in the experiment. The void fraction increased from 0 to 0.8 but could not increase indefinitely. There was no electrolyte flowing through the machining gap when the void fraction was close to 1; therefore, the machining process could not be completed. The experiments showed that the ECM became unstable, and an extreme short circuit occurred accompanied by a burning phenomenon when the void fraction exceeded 0.8. The relationship between the gas flow rate and the void fraction is illustrated in Fig. 8.

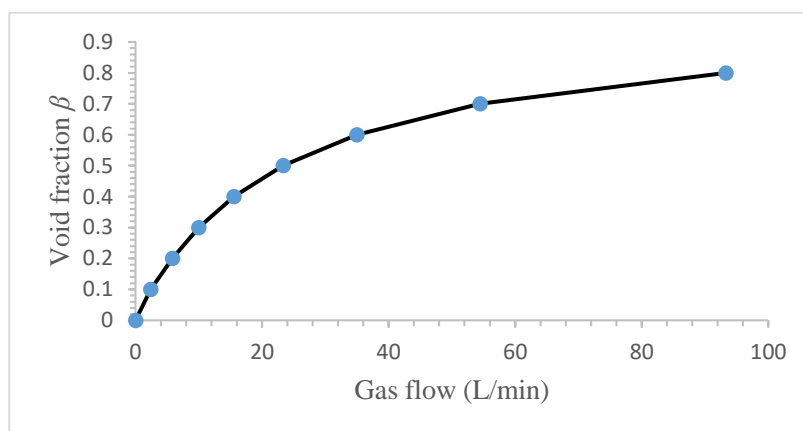


Figure 8. Relationship between gas flow and void fraction.

4.2 Effects of gas-mixed electrolyte flow on leveling ability

It is well known that gas mixed into the electrolyte of ECM has a significant influence on the electrolyte conductivity (κ). The value of electrolyte conductivity varied from 15 S/m to 2.46 S/m as the void fraction changed from 0% to 70% as shown in Table 2. Fig. 9 shows the variation curves of the final stepped height difference (δ_b), the dissolved depth (h), and the final machining gap (Δ_b) with a change in void fraction (β) obtained by the hex three coordinate measurement of the profile of a machined workpiece. It can be clearly seen that h and Δ_b declined significantly as β varied from 0% to 30%, and h decreased substantially when β exceeded 30%. This can be attributed to the electrolyte conductivity decreasing by 41% from 15 S/m to 8.78 S/m when the void fraction was less than 30%, and the electrolyte conductivity declining by 72% from 8.78 S/m to 2.46 S/m when the void fraction was greater than 30%. Moreover, δ_b reduced gradually when β was less than 40%, and δ_b increases slightly

when β was higher than 40%. This occurred because the electrolyte conductivity decreased as more gas was mixed into the electrolyte and decreased the material removal rate, especially when β was higher and the electrolyte conductivity was lower. Therefore, h reduced significantly and Δ_b increased slightly when β exceeded 40%. It can be calculated from Eq. (2) that the final machining gap decreased as more gas was mixed into the electrolyte. Hence, a small machining gap can be achieved when the gas is mixed into the electrolyte during ECM to obtain a more even electric field and flow field distribution and improve machining accuracy [12].

Table 2 Value of electrolyte conductivity with different void fractions

β	0	10%	20%	30%	40%	50%	60%	70%
K (S/m)	15	12.81	10.73	8.78	6.97	5.30	3.79	2.46

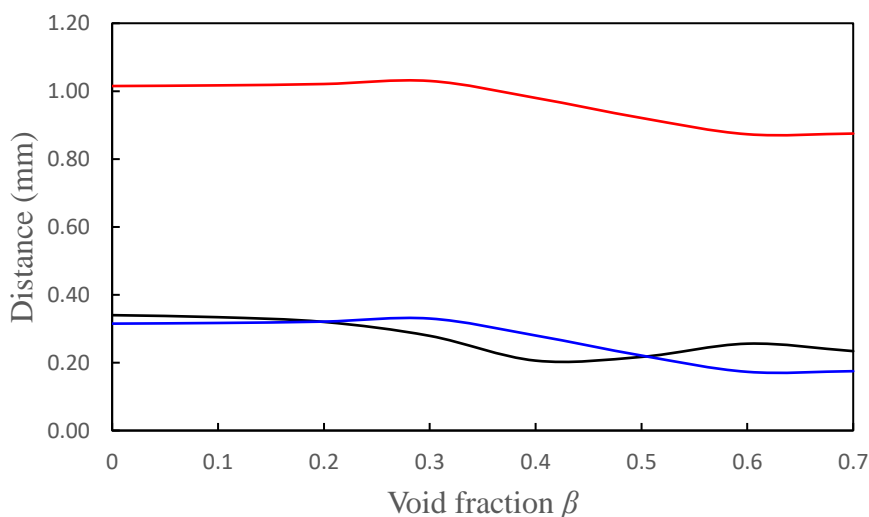


Figure 9. Relationship between δ_b , h , and Δ_b .

The leveling ability, which influences workpiece machining accuracy, is very crucial in the ECM process of profile machining. Fig. 10 illustrates the relationship between the leveling ratio, Ψ , and the void fraction, β . As shown, the leveling ratio increased slowly when the void fraction was less than 40% and significantly when the void fraction was greater than 40%. The maximum leveling ratio was close to 0.74 with a void fraction of 70%, but was only 0.49 with a void fraction of zero, thus demonstrating an increase in leveling ability of almost 51%.

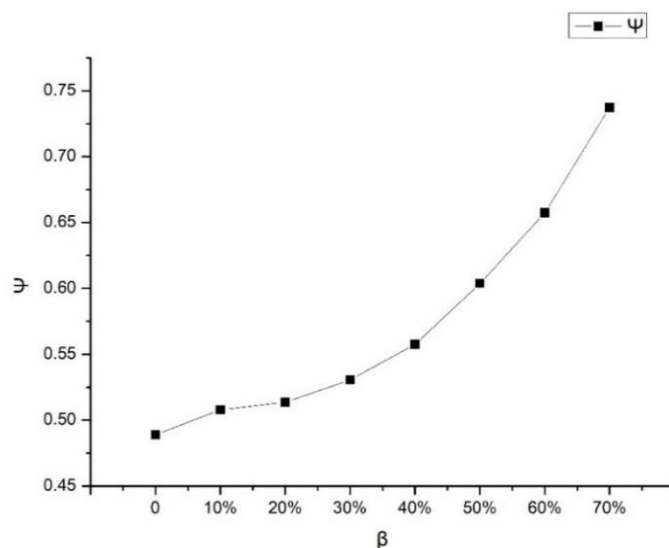
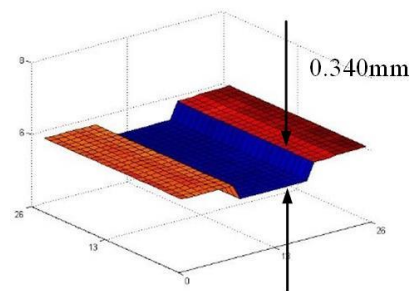
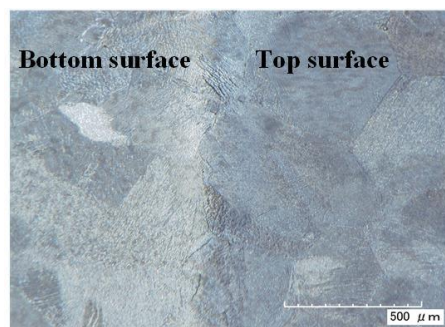


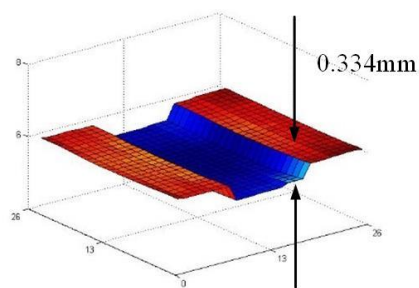
Figure 10. Relationship between leveling ratio, Ψ , and void fraction, β .

The high-speed camera observations and experimental results showed a larger amount of gas in larger machining gaps than in smaller machining gaps, and the diameter of bubbles in larger machining gaps was greater than that in smaller machining gaps. This phenomenon led to the electrolyte conductivity in a larger machining gap being lower than that in a smaller machining gap, and the material removal rate in a smaller machining gap was greater than that in a larger machining gap. Hence, the leveling ratio was reduced and the leveling ability enhanced with an increase in the void fraction. In addition, a smaller machining gap can be generated because the electrolyte conductivity decreases as more gas is mixed into the electrolyte. It is well known that a smaller ECM gap can improve machining accuracy and leveling ability. Therefore, gas-mixed electrolyte can improve the leveling ability and reduce the genetic error for profile ECM.

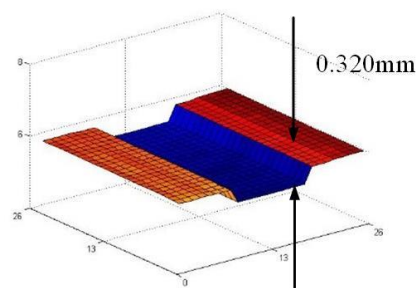
The top view optical images of the machined workpiece surface are displayed in Fig. 11. The step on the workpiece surface was clearly discernable when the void fraction was 0. The fitting profiles of the workpieces dissolved at different void fractions are also shown in Fig. 11, where the stepped height difference varied from 0.340 mm to 0.234 mm as the void fraction increased from 0% to 40%, and the stepped height difference changed from 0.234 mm to 0.204 mm as the void fraction varied from 40% to 70%. This is attributed to the sharp decrease in electrolyte conductivity when the void fraction was greater than 40%, and the material removal rate declined rapidly; therefore, the stepped height difference increased slightly with an increase in the void fraction from 40% to 70%.



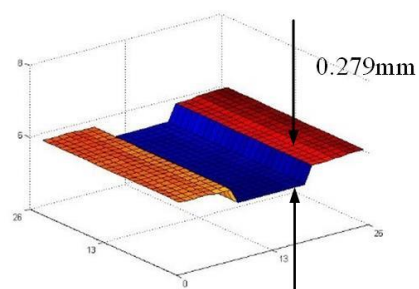
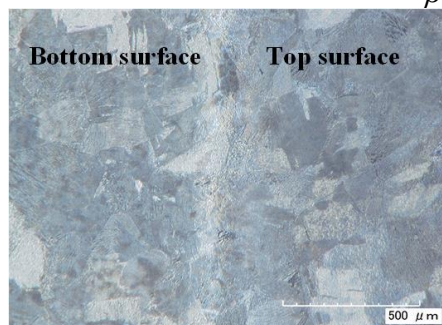
$\beta = 0$



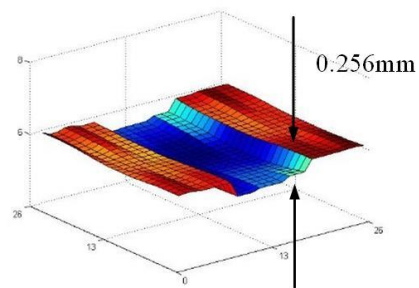
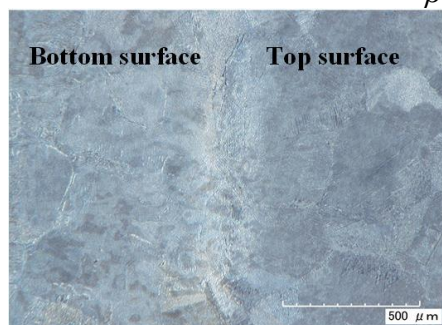
$\beta = 10\%$



$\beta = 20\%$



$\beta = 30\%$



$\beta = 40\%$

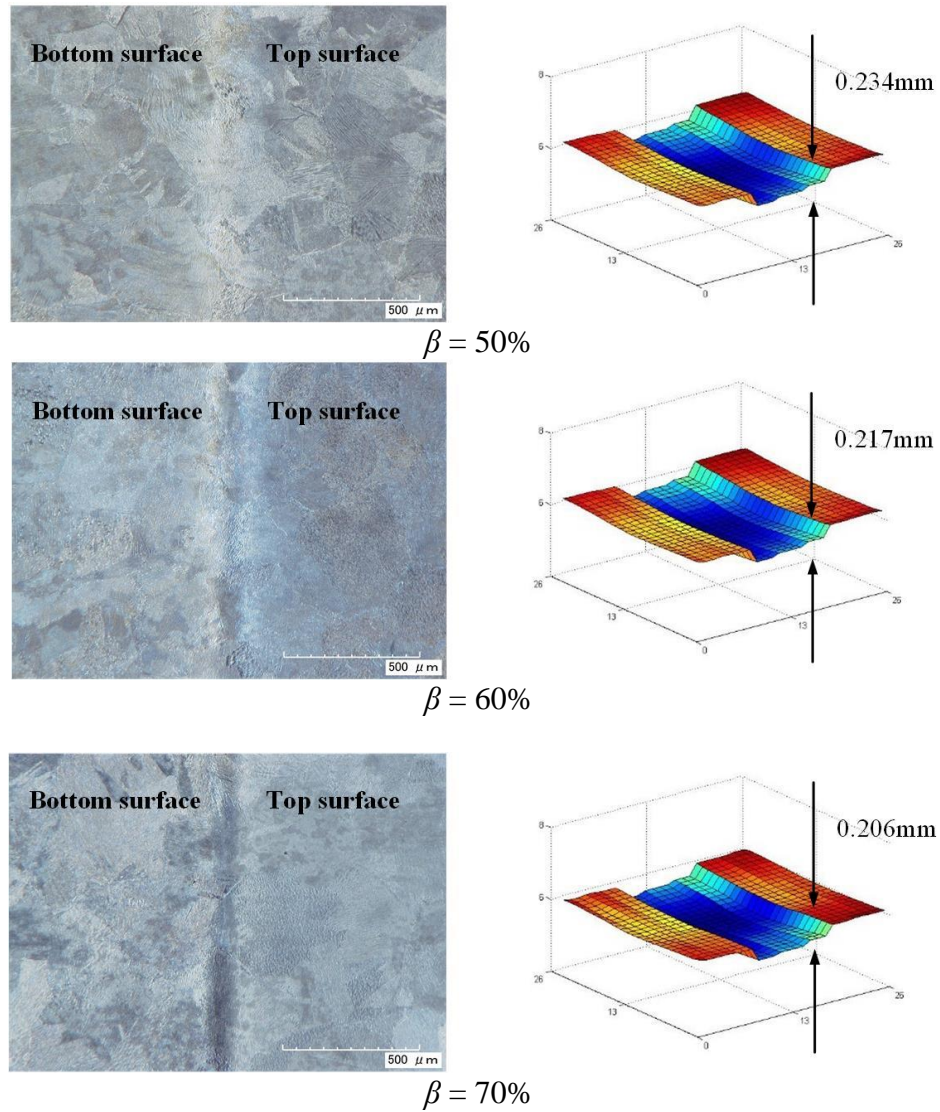


Figure 11. Optical images and fitting profiles of workpieces dissolved at different void fractions.

4.3 Effects of gas-mixed electrolyte flow on surface quality

To explore the effects of gas-mixed electrolyte flow on surface quality, the roughness of the machined surface profile near the center of a workpiece was measured as shown in Fig. 12.

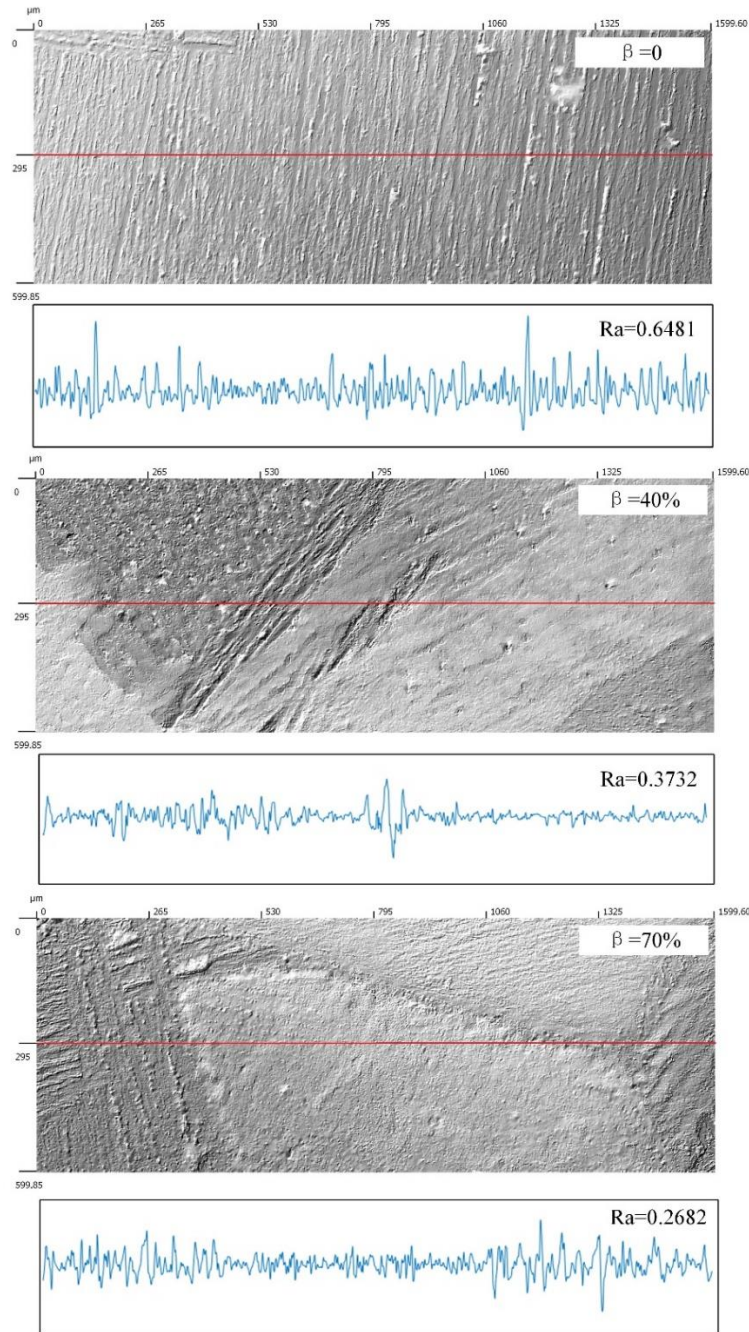


Figure 12. Roughness values at center of machined higher surface under different void fractions.

The surface topography became smoother with low surface roughness, and the roughness value was reduced from 0.6481 to 0.2682 when the void fraction changed from 0% to 70%. The results showed that the surface roughness of the gas-mixed ECM was better than that of traditional machining. In the gas-mixed ECM, the flow velocity of the electrolyte was greater, which can degrade the electrolytic products and the heat generated in the ECM process more quickly. Furthermore, a faster electrolyte flow can improve the uniformity of the flow field in the machining gap and improve the surface quality.

The results also indicated that with an increase in the void fraction, the smoothing effect on roughness became weaker. When the void fraction was 0.4, the surface roughness improved by 42.4% compared to a void fraction of 0. When the void fraction was 0.7, the surface roughness improved by

58.6% compared to a void fraction of 0. The reason for this phenomenon is that compared with traditional ECM, gas-mixed ECM significantly improves the electrolyte flow field; however, for gas-mixed ECM with different void fractions, the improvement of void fraction can only change the quality of the flow field, not the type of the flow field

Our study quantified the relationship between void fraction and leveling ratio and analyzed the influence of the use of gas-mixed electrolyte on ECM. The effect of adding compressed air to ECM was mentioned in related research. Hu used compressed air to create an air film isolation layer to protect the electrolytic non-processing area and decrease stray corrosion [14]. Ghabrial conducted experiments on conventional ECM and gas-mixed ECM under different operating conditions, and the experimental results showed that gas-mixed electrolyte improved the surface quality of a workpiece and the processing stability [15]. Peng conducted experiments and found that gas-mixed ECM reduced the machining gap and improved the machining and replication accuracies [16].

5. CONCLUSION

Gas-mixed electrolyte flow was introduced to improve the leveling ability and surface quality for the ECM of ($\gamma+\alpha_2+B_2$) TiAl intermetallic. The conclusions can be summarized as follows:

1. High-speed camera observations showed the existence of greater amounts of gas in larger machining gaps than in smaller machining gaps. In addition, the diameter of bubbles in larger machining gaps is greater than that in smaller machining gaps and leads to greater electrolyte conductivity, and the material removal rate in smaller machining gaps is higher than that in larger machining gaps.

2. The leveling ratio increased from 0.49 to 0.74 when the void fraction increased from 0% to 70%, and the leveling ability increased by almost 51%, which verified that a higher leveling ability was obtained by using gas-mixed electrolyte during ECM.

3. The surface roughness of the workpiece was improved by the addition of greater amounts of gas mixed into the electrolyte. The roughness decreased from 0.6481 to 0.2682 when the void fraction increased from 0% to 70%. Therefore, the surface quality was improved by using gas-mixed electrolyte in the ECM.

ACKNOWLEDGMENTS

The authors acknowledge the financial support provided by the National Natural Science Foundation (U1601201), the Natural Science Foundation for Distinguished Young Scholars of Jiangsu Province of China (BK20170031), and the Research Innovation Program for College Graduates of Jiangsu Province (Grant No. KYLX15_0289).

References

1. K. P. Rajurkar, D. Zhu, J. A. McGeough, J. Kozak, A. D. Silva, *Cirp Annals.*, 48 (1999) 567.
2. V. V. Lyubimov, V. M. Volgin, V. P. Krasilnikov, *Int. Conf. Ind. Eng.*, (2019) 391.
3. K. P. Rajurkar, D. Zhu, B. Wei. *Cirp Annals.*, 47 (1998) 165.
4. D. Zhu, Y. W. Zhou, R. H. Zhang, P. Qin. *Int. J. Adv. Manuf. Tech.*, 86 (2016) 1723.

5. Y. Li, Y. F. Zheng, G. Yang, L. Q. Peng, *Sensor. Actuat. A-Phys.*, 108 (2003) 144.
6. D. Bähre, A. Rebschläger, O. Weber, P. Steuer, *Procedia Cirp.*, 6 (2013) 384.
7. S. Q. Qian, F. Ji, N. S. Qu, H. S. Li, *Mater. Manuf. Process.*, 29 (2014) 1488.
8. Z. Y. Li, X. T. Wei, W. W. Lu, Q. W. Cui, *Appl. Mech. Mater.*, 868 (2017) 166.
9. X. Y. Hu, D. Zhu, J. B. Li, Z. Z. Gu, *J. Mater. Process. Tech.*, 267 (2019) 247.
10. S. Ayyappan, K. Sivakumar, *Int. J. Adv. Manuf. Tech.*, 75 (2014) 479.
11. Z. Y. Xu, Y. D. Wang, *Chinese. J. Aeronaut.*, (2019).
12. J. W. Xu, Y. Q. Wang, X. J. Deng, C. Y. Yu, *Trans. Nanjing. U. Aeronaut. Astronaut.*, 4 (1996) 4.
13. F. Klocke, M. Zeis, T. Herrig, S. Harst, A. Klink, *Procedia Cirp.*, 24 (2014) 114.
14. X. Y. Hu, D. Zhu, J. B. Li, Z. Z. Gu, *J Mater Process Tech.*, 267 (2019) 247.
15. S. R. Ghabrial, S. J. Ebeid, *Precis Eng.*, 3 (1981) 221.
16. J. Peng, M. H. Jia, J. Meng, *Machinery*, 5 (2010) 22.

© 2020 The Authors. Published by ESG (www.electrochemsci.org). This article is an open access article distributed under the terms and conditions of the Creative Commons Attribution license (<http://creativecommons.org/licenses/by/4.0/>).